Mechanics of Advanced Composite Structures 10 (2023) 309 – 318

Semnan University

Mechanics of Advanced Composite Structures

journal homepage: http://MACS.journals.semnan.ac.ir

Minimal Mass and Maximal Buckling Load of Composite Hexagonal-Triangle Grid Structure using FSDT under External Hydrostatic Pressure

M. Soheil Shamaee [a*], A.R. Ghasemi [b]

[a] *Department of Computer Science, Faculty of Mathematical Sciences, University of Kashan, Kashan 87317-53153, I. R. Iran*
[b] *Composite and Nanocomposite Research Laboratory, Department of Solid Mechanics, Faculty of Mechanical Engineering, University of Kashan, Kashan, 87317-5315, Iran*

KEYWORDS

Grid stiffeners;
Buckling load;
Composite shell;
Optimization;
Genetic algorithm.

ABSTRACT

Grid-stiffened composite shells are one of the most important structures in many industries. These structures based on their fabrication method, provide both high strength and light structural weight. In this study, buckling analysis under external hydrostatic pressure is performed to obtain critical buckling pressure and the optimum values of parameters for stiffeners. First-order shear deformation theory (FSDT) based on the Ritz method is used to calculate the critical buckling load of these structures. The effects of shell thickness, angle of helical stiffeners, rib section area, and the stiffeners number into the buckling load are determined. Comparing the calculated buckling load for stiffened and non-stiffened structures shows that stiffeners significantly optimize structural performance. Furthermore, optimization of stiffener parameters is done by Genetic Algorithm. The results show that the introduced structure has the minimum mass. So, the stiffener parameters would be better. According to the results, the optimum dimensions for stiffener buckling load for the optimal stiffener have been increased by about 80% compared to non-stiffened.

1. Introduction

A composite grid structure is a structure of composite one-directional tapes that are joined together to form a continuous set as two-dimensional (planar) or three-dimensional (spatial). Composite grid structures are more capable than metal structures due to strength, low weight, flexibility in design, easy construction, and the ability to withstand various environmental conditions. Shells that have been stiffened with grid structures are an appropriate alternative for composite, sandwich, or filled metal panels. The main objective of using grid structures is the optimization of longitudinal properties of composite materials in structures. Although grid structures are being used as a new technology in many industries, especially the aerospace industry. However, in the past, several valuables of research have been conducted on this kind of structure.

Genetic algorithm (GA) as an evolutionary approach is suitable for tackling optimization problems. Many researchers reported that GA has a good performance to find the near-optimal solutions of discrete optimization problems such as composite structures [1-4].

Kim [5] studied the construction of composite grid cylinders, in which building and buckling strength analysis of a stiffened cylinder with the same grid were studied. He investigated the effects of a vertical compressive force on the buckling and rib failure and stability of the entire structure have been studied. In [5], he focused on grid composite panels instead of grid cylinders and examined buckling modes, rib failure, shell, and the entire structure failure. Authors in [6] studied the optimization of a rotating structure with variable curvature. This structure was composed of a shell and a composite grid structure. The purpose of that optimization problem was to minimize the weight of this structure, so that with the change in the size and rib spacing, this structure had the lowest weight, and also required strength under local buckling.

After that, Zhang et al. [7] published an article in which they introduced two new grid structures and calculated their mechanical properties.

* Corresponding author. Tel.: +98-31-55913048 ; Fax: +98-31-55912501
E-mail address: soheilshamaee@kashanu.ac.ir

DOI: 10.22075/macs.2023.28896.1450
Received 2022-11-05; Received in revised form 2023-01-06; Accepted 2023-01-10

These two structures were a combination of known structures. They also validated the obtained properties for these structures with the finite element method. Yazdani et al. [8] performed an experimental study on the composite grid shells buckling under axial load. They concluded that increasing the number of helical ribs has more effective than adding circumferential rings or changing the grid type. On the other hand, shells with diamond-shaped grids had a more favorable performance in axial loading [8].

Jingxuan et al. [9] placed an advanced grid stiffened (AGS) composite under axial load. They determined the structural strength and failure threshold of the structure. The results were compared with the finite element method by ANSYS commercial software. Other researchers [10] explained the grid composite structures, their construction process, and the latest achievements and their applications in the space industry. In this study, ribs in the grid structure strengthen the structure and reduce its weight.

Rahimi et al. [11] implemented and evaluated a grid composite cylinder with ANSYS commercial software. They examined the effect of the rib profile on the cylinder resistance under axial pressure load by changing the cylinder diameter and rib profile. Weber and Middendorf [12] integrated the interaction between adjacent skin fields into the calculation of the local skin buckling load by applying periodic boundary conditions at opposite panel edges. They considered the self-stiffening effect of the grid-stiffened structures due to interaction with adjacent skin fields, significantly increasing the buckling resistance of such structures.

Liu and Paavola [13] evaluated a general analytical sensitivity analysis method for the composite laminated panels and shells. This method is applied to both classical laminate plate theory (CLPT) and first-order shear deformation theory (FSDT) based on the finite element methods. Deveci [14] optimized the buckling of the composite laminates using a hybrid algorithm under the Puck failure criterion constraint. They proposed an optimization method to find the optimum stacking sequence designs of laminated composite plates in different fiber angle domains for maximum buckling resistance.

Civalek [15] worked on buckling analysis of the composite shells with different material properties by the discrete singular convolution (DSC) method. Ghasemi et al. [16] presented a multi-objective optimization of a composite cylindrical shell under external hydrostatic via an improved version of the evolutionary algorithm of NSGA-II. The parameters of mass, cost, and buckling pressure as fitness functions and failure criteria as optimization criteria were considered. Also, the kind of material, the number of layers, and fiber orientations have been considered as design variables.

Hajmohammad et al. [17] developed a practical analytical approach to reach the optimal fiber orientation in the design of fiber-reinforced polymer pressure vessels (FRPPVs) subjected to hydrostatic pressure. The genetic algorithm (GA) is applied to achieve the optimal orientation pattern with minimum weight and maximum buckling load.

Ghasemi et al. [18] presented a multi-step optimization method to predict the optimal fiber orientation in glass fiber-reinforced polymer (GFRP) composite shells. The proposed method contains a regenerated genetic algorithm (GA) coupled with an analytical approach to assessing the failure of the tubular structure.

Soltani et al. [19] investigated the lateral buckling analysis and layup optimization of the laminated composite of web and flanges tapered thin-walled I-beams based on maximizing lateral-torsional stability strength and minimizing the mass of the structure. The critical factors of fitness function as lateral buckling strength and the mass of the structure with critical limitations such as ply angle, number of layers for the web and flanges, and the thickness of all section walls are considered to be optimized using the non-dominated sorting genetic algorithm (NSGA-II) and properly defined objective function.

The natural frequency analysis of vertical functionally graded (FG) microplates partially in contact with fluid was investigated by Khorshidi et al [20]. Thermal buckling, bending, and free vibration analyses of micro-scaled functionally graded GNPs reinforced porous nanocomposite annular plate were considered by Amir et al [21].

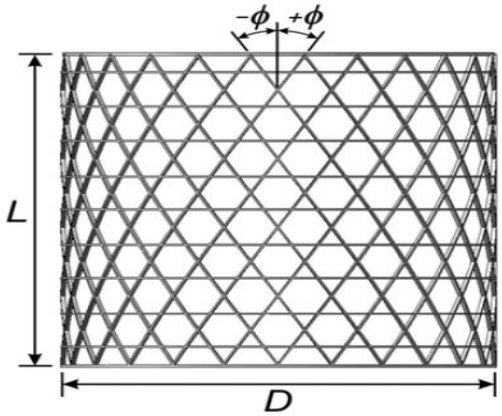

Fig. 1. Grid cylindrical shell

The study aims to gain the critical buckling pressure for grid composite structures under external hydrostatic pressure. In this study, a stiffened composite cylindrical shell using a grid structure with internal stiffeners hexagonal -

triangle grid under external hydrostatic pressure is analyzed. With the development of smeared method and also using the linear FSDT, buckling critical pressure can be calculated. By calculating the critical buckling pressure for different modes, the effect of stiffener parameters on buckling pressure can be obtained. Moreover, given that in many industries, the use of lighter structures is in priority, grid structures were optimized to reduce weight, and identify the optimal dimensions of stiffeners in this certain problem. In the end, the optimization of composite grid shells was designed using a Genetic Algorithm (GA) and the optimum parameters of stiffeners are introduced. Two scenarios of GA based on their population size and iteration number were performed to obtain the optimized parameters.

2. Equations and Assumptions

Figure 1 shows a cylindrical shell stiffened by grid stiffeners. This shell has length L, thickness t, and diameter D. The following assumptions were considered in this structure:

1. The shell was considered thin and a composite laminate.
2. Each rib of stiffeners is a thin laminated panel that is formed from layers with continuous fibers and a single direction.
3. The used theory is the first-order shear deformation theory.
4. Stiffeners have been considered internally and the entire structure is under external hydrostatic pressure and the load is applied from the side.
5. Rib cross-sections of stiffeners are considered rectangular.
6. Stiffeners arrangement is the hexagonal-triangle combination.

Displacements are provided by the FSDT in cylindrical coordinates in the below equations, that u, v, and w are displacement components at any arbitrary point of the shell, u_0,v_0, and w_0 are the displacement components in the middle level, ψ_x and ψ_θ are rotation from θ and x-axis, respectively [22].

$$u(x,\theta,z) = u_0(x,\theta) + z\,\psi_x(x,\theta) \quad (1)$$

$$v(x,\theta,z) = v_0(x,\theta) + z\,\psi_\theta(x,\theta) \quad (2)$$

$$w(x,\theta,z) = w_0(x,\theta) \quad (3)$$

3. Making the Equivalent of Composite Grid Shells

Smeared method for evaluating interactions between the shell and the stiffener was presented by Jaunky et al. [23]. Kidane et al. [24] have provided a method to study the axial buckling of the grid composite cylinder by using the same theory. To make the equivalent of stiffeners, strains and forces in the stiffeners are calculated. Then, by considering the stiffness matrix obtained for stiffeners, a shell with appropriate thickness is determined which has stiffness exactly equal to stiffeners. At this step, determining shell is replaced instead of the total stiffeners, and finally, the shell is added to the primary shell, and all of them are considered as a structural unit.

3.1. Force Analysis in the Stiffeners

$$\begin{cases} \varepsilon_{xx} = \varepsilon_{xx}^{(0)} + (\frac{t}{2})k_{xx} \\ \varepsilon_{\theta\theta} = \varepsilon_{\theta\theta}^{(0)} + (\frac{t}{2})k_{\theta\theta} \\ \gamma_{x\theta} = \gamma_{x\theta}^{(0)} + (\frac{t}{2})k_{x\theta} \end{cases} \quad (4)$$

$$\begin{cases} \gamma_{xz} = \gamma_{xz}^{(0)} \\ \gamma_{\theta z} = \gamma_{\theta z}^{(0)} \end{cases} \quad (5)$$

By loading the entire structure, reaction forces in stiffeners are made as an axial force in the stiffeners section which is shown with F_l. However, during this loading, stiffeners can bear shear loads and planar shear loads, which are expressed with F_{lt} and F_{lz}, respectively. Inside axial and shear forces applied to the stiffeners are shown in Fig.2.

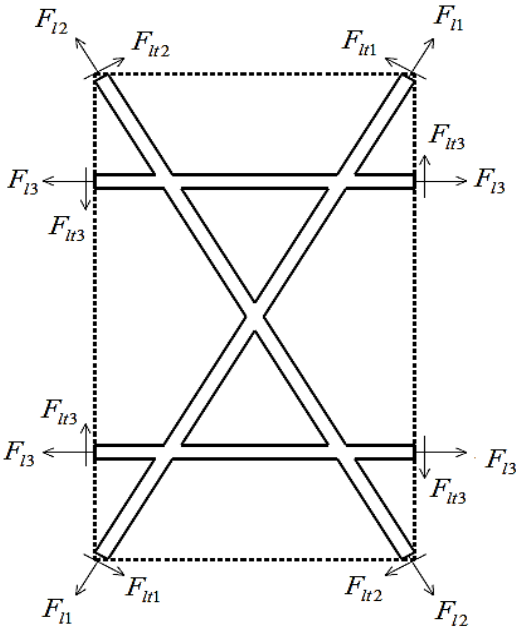

Fig. 2. Forces applied to the stiffeners

By solving the strains in the direction of stiffeners and the perpendicular on stiffeners, stiffeners forces are obtained concerning strains.

$$F_{l1} = A_{st}E_l\varepsilon_{l1} = A_{st}E_l(c^2\varepsilon_{xx} + s^2\varepsilon_{\theta\theta} - cs\gamma_{x\theta}) \quad (6)$$

$$F_{l2} = A_{st}E_l\varepsilon_{l2} = A_{st}E_l \times (c^2\varepsilon_{xx} + s^2\varepsilon_{\theta\theta} + cs\gamma_{x\theta}) \quad (7)$$

$$F_{l2} = A_{st}E_l\varepsilon_{l3} = A_{st}E_l(\varepsilon_{\theta\theta}) \quad (8)$$

3.2. Moment Analysis of the Stiffener

Moments applied to the stiffeners at the interface between the shell and stiffener, are caused due to shear forces. Moments applied to the unit cell are shown in Fig.3.

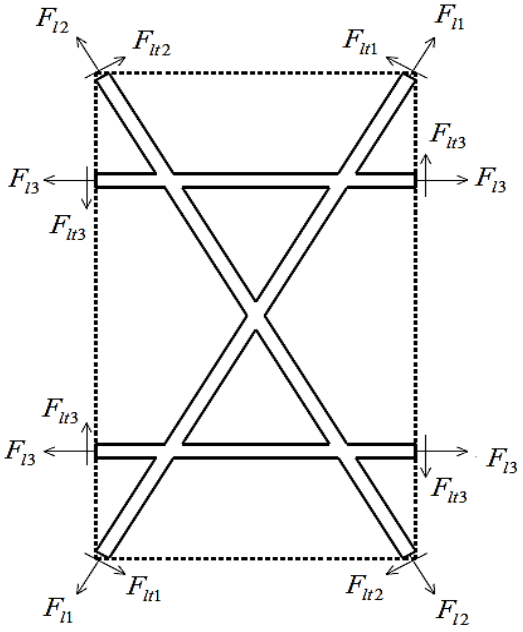

Fig. 3. Moments applied to the stiffeners

According to the presented method in the previous section, the applied moment on the sides of the unit cell can be obtained as equations (9), (10), and (11).

$$M_x = \begin{pmatrix} \frac{2A_{st}E_lc^3}{a}\varepsilon_{xx} + \frac{2A_{st}E_lcs^2}{a}\varepsilon_{\theta\theta} + \\ \frac{2A_{st}G_{lt}sc^2}{a}\gamma_{x\theta} - \frac{2A_{st}G_{lt}s^3}{a}\gamma_{x\theta} \end{pmatrix}\left(\frac{t+h}{2}\right) \quad (9)$$

$$M_\theta = \begin{pmatrix} \frac{2A_{st}E_lsc^2}{b}\varepsilon_{xx} + \frac{2A_{st}E_l\left(s^3+1\right)}{b}\varepsilon_{\theta\theta} \\ -\frac{2A_{st}G_{lt}c^3}{b}\gamma_{x\theta} + \frac{2A_{st}G_{lt}cs^2}{b}\gamma_{x\theta} \end{pmatrix}\left(\frac{t+h}{2}\right) \quad (10)$$

$$M_{x\theta} = \begin{pmatrix} -\frac{4A_{st}G_{lt}cs^2}{b}\varepsilon_{xx} + \frac{4A_{st}G_{lt}cs^2}{b}\varepsilon_{\theta\theta} \\ +\frac{2A_{st}E_lsc^2}{b}\gamma_{x\theta} \end{pmatrix}\left(\frac{t+h}{2}\right) \quad (11)$$

By taking a plane with normal vector Z, components of shear strains ε_{lz} are:

$$\varepsilon_{lz} = (s\gamma_{\theta_z} + c\gamma_{xz}) \quad (12)$$

The shear forces caused by shear strains are obtained as follows:

$$F_{lz1} = A_{st}G_{lz}\gamma_{lz1} = A_{st}G_{lz}(-s\gamma_{\theta_z} + c\gamma_{xz}) \quad (13)$$

$$F_{lz2} = A_{st}G_{lz}\gamma_{lz2} = A_{st}G_{lz}(s\gamma_{\theta_z} + c\gamma_{xz}) \quad (14)$$

$$F_{lz3} = A_{st}G_{lz}\gamma_{lz3} = A_{st}G_{lz}(\gamma_{\theta_z}) \quad (15)$$

By analyzing the forces, moments, and shear forces exerted on the unit cell transforming from these equations as matrix multiplication, stiffness matrix can be achieved as shown in equation (16). Since the shell is a laminated composite, the shell stiffness matrix can be written as equation (17) [25-26].

It is noteworthy that the axial stiffness A_{ij}, coupled stiffness (bending-axial) B_{ij}, bending stiffness D_{ij} and shear stiffness H_{ij} are obtained via the equations (18), (19), (20), and (21) where K_0 is the shear correction factor with the amount of $\frac{5}{6}$ [22].

Finally, the equivalent stiffness matrix for a composite grid shell is the sum of the shell stiffness matrix and the stiffeners stiffness matrix as shown in the equation (22).

$$\begin{bmatrix} N_x \\ N_\theta \\ N_{x\theta} \\ M_x \\ M_\theta \\ M_{x\theta} \\ Q_x \\ Q_\theta \end{bmatrix} = \begin{bmatrix} A_{11}^{st} & A_{12}^{st} & A_{13}^{st} & B_{11}^{st} & B_{12}^{st} & B_{13}^{st} & 0 & 0 \\ A_{21}^{st} & A_{22}^{st} & A_{23}^{st} & B_{21}^{st} & B_{22}^{st} & B_{23}^{st} & 0 & 0 \\ A_{31}^{st} & A_{32}^{st} & A_{33}^{st} & B_{31}^{st} & B_{32}^{st} & B_{33}^{st} & 0 & 0 \\ B_{11}^{st} & B_{12}^{st} & B_{13}^{st} & D_{11}^{st} & D_{12}^{st} & D_{13}^{st} & 0 & 0 \\ B_{21}^{st} & B_{22}^{st} & B_{23}^{st} & D_{21}^{st} & D_{22}^{st} & D_{23}^{st} & 0 & 0 \\ B_{31}^{st} & B_{32}^{st} & B_{33}^{st} & D_{31}^{st} & D_{32}^{st} & D_{33}^{st} & 0 & 0 \\ 0 & 0 & 0 & 0 & 0 & 0 & H_{44}^{st} & H_{45}^{st} \\ 0 & 0 & 0 & 0 & 0 & 0 & H_{44}^{st} & H_{45}^{st} \end{bmatrix} \begin{bmatrix} \varepsilon_{xx}^{(0)} \\ \varepsilon_{\theta\theta}^{(0)} \\ \varepsilon_{x\theta}^{(0)} \\ k_{xx} \\ k_{\theta\theta} \\ k_{x\theta} \\ \gamma_{xz}^{(0)} \\ \gamma_{\theta z}^{(0)} \end{bmatrix} \tag{16}$$

$$S_{sh} = \begin{bmatrix} A_{11} & A_{12} & A_{13} & B_{11} & B_{12} & B_{13} & 0 & 0 \\ A_{21} & A_{22} & A_{23} & B_{21} & B_{22} & B_{23} & 0 & 0 \\ A_{31} & A_{32} & A_{33} & B_{31} & B_{32} & B_{33} & 0 & 0 \\ B_{11} & B_{12} & B_{13} & D_{11} & D_{12} & D_{13} & 0 & 0 \\ B_{21} & B_{22} & B_{23} & D_{21} & D_{22} & D_{23} & 0 & 0 \\ B_{31} & B_{32} & B_{33} & D_{31} & D_{32} & D_{33} & 0 & 0 \\ 0 & 0 & 0 & 0 & 0 & 0 & H_{44} & H_{45} \\ 0 & 0 & 0 & 0 & 0 & 0 & H_{54} & H_{55} \end{bmatrix} \tag{17}$$

$$A_{ij} = \int_{-\frac{h}{2}}^{\frac{h}{2}} Q_{ij} dz \rightarrow A_{ij} = \sum_{k=1}^{N_l} \overline{Q}_{ij}^{\,k} (h_k - h_{k+1}) \qquad i,j = 1,2,6 \tag{18}$$

$$B_{ij} = \frac{1}{2} \int_{-\frac{h}{2}}^{\frac{h}{2}} Q_{ij} z dz \rightarrow B_{ij} = \sum_{k=1}^{N_l} \overline{Q}_{ij}^{\,k} z (h_k^2 - h_{k+1}^2) \qquad i,j = 1,2,6 \tag{19}$$

$$D_{ij} = \frac{1}{3} \int_{-\frac{h}{2}}^{\frac{h}{2}} Q_{ij} z^2 dz \rightarrow D_{ij} = \sum_{k=1}^{N_l} \overline{Q}_{ij}^{\,k} z^2 (h_k^3 - h_{k+1}^3) \qquad i,j = 1,2,6 \tag{20}$$

$$H_{ij} = K_0 \int_{-\frac{h}{2}}^{\frac{h}{2}} Q_{ij} dz \rightarrow H_{ij} = K_0 \sum_{k=1}^{N_l} \overline{Q}_{ij}^{\,k} (h_k - h_{k+1}) \qquad i,j = 4,5 \tag{21}$$

$$S = S_{\text{sh}} + S_{st} \tag{22}$$

3.3. Analysis of Buckling Load by Rayleigh-Ritz method

In the Ritz method, the total energy function (Π) is achieved from the sum of the values of strain energy and work done by external forces. On the other side, to create balance, the total energy function of the structure must be minimized. In other words, to minimize the total energy, total potential energy should be differentiated concerning displacement field coefficients A_{mn}, B_{mn} and C_{mn}, and by putting them equal to zero, the coefficient matrix is obtained [27-28]:

$$\Pi = U + V \tag{23}$$

$$\frac{\partial \Pi}{\partial A_{mn}} = \frac{\partial \Pi}{\partial B_{mn}} = \frac{\partial \Pi}{\partial C_{mn}} = 0 \quad (24)$$

$$\begin{bmatrix} L_{11} & L_{12} & L_{13} \\ L_{21} & L_{22} & L_{23} \\ L_{31} & L_{32} & L_{33} \end{bmatrix} \begin{bmatrix} A_{mn} \\ B_{mn} \\ C_{mn} \end{bmatrix} = 0 \quad (25)$$

To have non-trivial solutions in the above equation, the determinant of the coefficient matrix must be zero ($|L_{ij}| = 0$). After the extension of this equation, the buckling characteristic equation is obtained, and by solving this equation, the buckling load for the different m and n is achieved. It should be noted that the minimum amount of P, is the buckling critical load.

4. Results and Discussion

4.1. Validation

We have verified the results caused by the buckling of composite cylindrical shells with those of reference [29]. We have considered a cylindrical shell with a 200 mm diameter and 600 mm lengths. The mechanical properties of shell material (without stiffeners) are provided in Table 1. Also, the layers' angle is [90/60/45]sym.

Table 1. Mechanical properties of the shell material

Properties
$E_{11} = 17.8(GPa)$
$G_{12} = 3.6(GPa)$
$G_{13} = 3.6(GPa)$
$\rho = 1800(kg/m^3)$
$E_{22} = 4.2(GPa)$
$G_{23} = 2.1(GPa)$
$v_x = 0.274$

Figure 4 shows the buckling load for a shell with and without stiffeners based on the thickness. The obtained results demonstrate that using grid stiffeners for all shells (with different thicknesses) increases buckling load.

4.2. The Effect of Stiffener Angle

Figure 5 shows the buckling load and specific buckling load concerning the helical rib angle for three different thicknesses. As can be seen, by increasing the helical rib angle for each thickness, the buckling load first is increased, and then after a certain angle (about 75 to 85 degrees) is reduced.

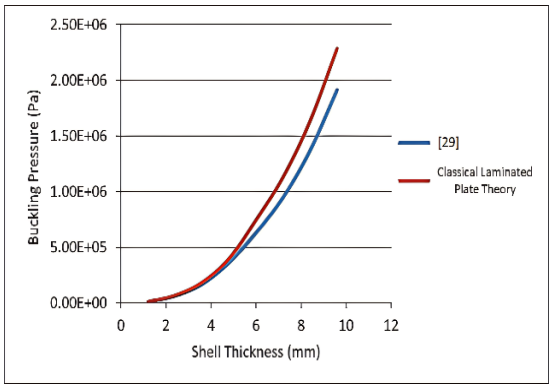

Fig. 4. Buckling load for a grid composite shell with and without stiffeners

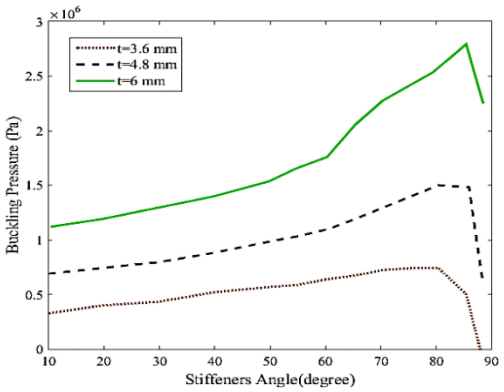

Fig. 5. The effect of stiffeners angle on the buckling load

4.3. The Effect of Rib Heights

Figure 6 shows the buckling load for different rib heights. It is evident that for all shell thicknesses, increasing the height of ribs increases the buckling load.

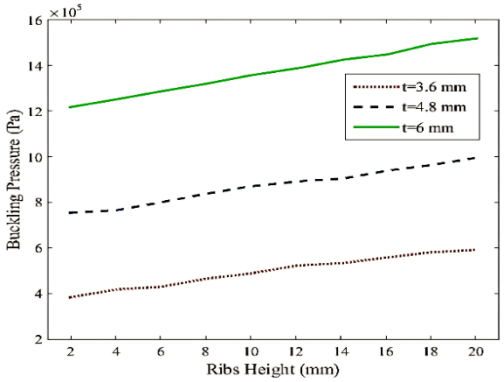

Fig. 6. The effect of rib height on the buckling load

4.4. The Effect of Rib Section Area

Figure 7 shows the effect of the rib section area on the buckling load. The results show that by increasing the stiffener section area, the buckling load increases, and the larger the ribs section area, the higher the buckling load.

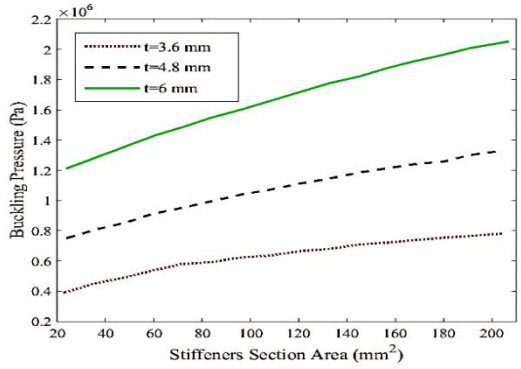

Fig. 7. The effect of the stiffeners section area on the buckling load

4.5. The Effect of Helical Stiffeners Number

Figure 8 shows the effect of the helical stiffener number on the buckling load. The results indicate that by increasing the number of helical stiffeners, the buckling load will be increased.

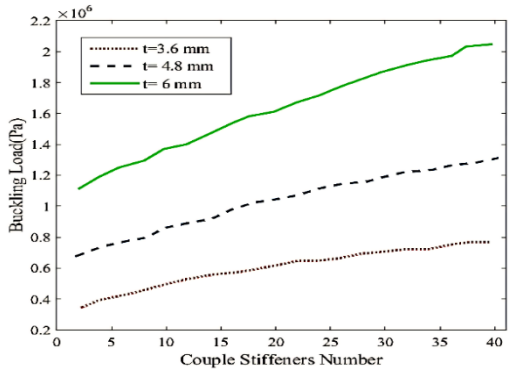

Fig. 8. The effect of a couple of stiffeners numbers on the buckling load

5. Optimization of Grid Shells Using Genetic Algorithm

Genetic algorithm, inspired by genetic science and Darwin's evolutionary theory, is based on natural selection. Genetic algorithms are commonly used to generate high-quality solutions to optimization problems. The Genetic Algorithm (GA) finds near-optimal solutions to problems by relying on operators such as mutation, crossover, and selection. Figure 9 shows the flowchart of GA with all steps involved from the beginning until the end.

To reduce the weight of our proposed composite grid shell by Genetic Algorithm, we should first determine the objective function based on the weight of the structure. Equation (26) presents the weight function, which is the sum of the stiffeners' weight and shell weight.

$$w_{tot} = w_{st} + w_{sh} = \rho\left(\left(2n_{st}l_{st}ft\right)+\left(2m_{st}\left(2\pi Rft\right)\right)\right)+\rho\left(2\pi RLh\right) \quad (26)$$

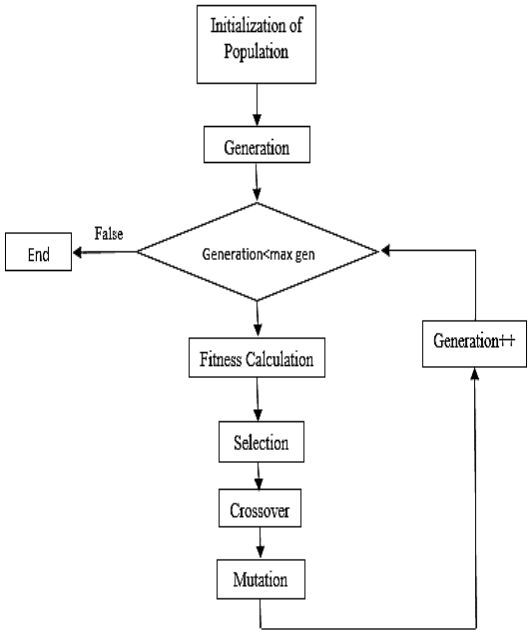

Fig. 9. Flowchart of Genetic Algorithm

The criterion of the optimization is buckling pressure. In this case study, the buckling pressure must not be more than 1 MPa. The buckling pressure could be obtained from the analytical solution in the previous section.

Since the weight function is a function of the shell parameters, so we also need to specify the variables. In this case, the couple number of helical stiffeners, the unit cell number in shell height, and also ribs thickness and width have been considered as the variables. Notably, lower and upper bounds for each variable were defined. In Table 2, variables are presented along with their upper and lower bounds.

Table 2. Variables and their ranges

Variable	Ranges
n_{st} : Couple helical stiffeners number	$2-12$
m_{st} : Unit cell number in height shell	$2-12$
$f(mm)$: Rib width	$2-12$
$t(mm)$: Rib thickness	$2-12$

Another point that should be addressed at the beginning of applying GA is the population size. In this study, the population size is considered between 15 and 20. The selection operator here is the Elitism operator.

According to the crossover, Mutation, and also elitism selection operators in the Genetic Algorithm, the parameters, the crossover probability, the mutation probability, and the elitism probability should be determined. The crossover possibility for each chromosome pair is considered 0.8. Also, the mutation probability

which is the probability of doing a jumping act on each chromosome is considered 0.2, and the elitism possibility which is defined as the probability of chromosome selection is considered 0.35.

5.1. First Scenario

In the first optimization scenario, the population size is intended 20 and also the algorithm is repeated 20 times. The results are shown in Fig.10 and Fig.11.

Figure 10 shows the optimization process of the structure mass in terms of the iteration numbers, and it consists of two data sets, which are the minimum mass and the average mass for each generation. According to this figure, it is clear that as the iteration progress, the structure mass decreases. Therefore, a near-optimal structure can be achieved.

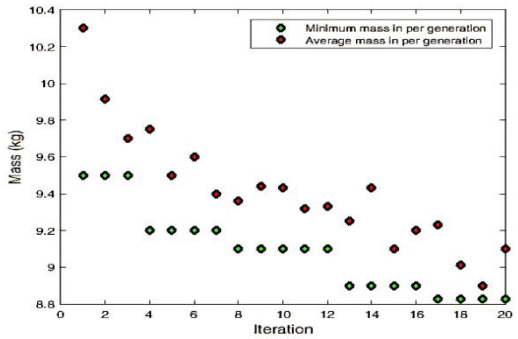

Fig. 10. Optimization process of the structure mass in terms of algorithm iterations (first scenario)

Figure 11 shows the minimum mass of the structure for each generation in terms of iteration in a separate form. In this figure, the optimization process is more evident.

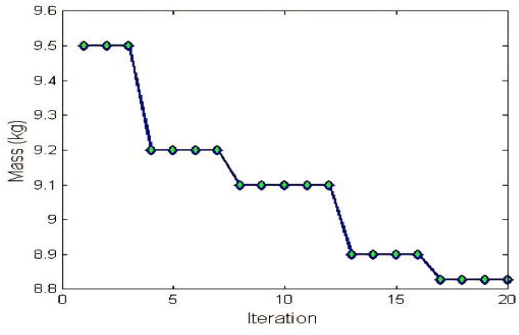

Fig. 11. The structure mass in terms of iterations (first scenario)

5.2. Second Scenario

In the second optimization scenario, the population size is 15 and the iteration number is 30. The results are shown in Fig.12 and Fig.13. the aim of this scenario is studying about the effects of increasing the number of interactions on the optimal solution found by the applied GA.

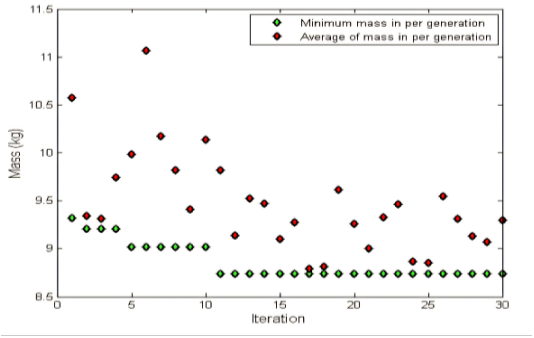

Fig. 12. Optimization process of the structure mass in terms of algorithm iterations (second scenario)

Figure 12 shows the optimization process of the structure mass in terms of the iteration number, with the difference that the iteration number has increased compared to the first scenario. As can be seen, the more iteration number, the less amount of the mass for each generation. So, by repeating the algorithm, a better solution can be achieved.

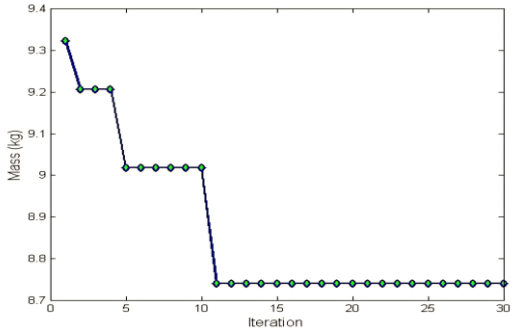

Fig. 13. The structure mass in terms of iterations (second scenario)

Figure 13 shows the minimum mass of the structure for each generation, in terms of the iteration number. As can be seen, the applied GA converges and the minimum mass has not changed for generations 11 to 30 and is a fixed value.

Table 3. The stiffeners' optimum size

Scenario Number	$m(kg)$	φ	$t(mm)$	$f(mm)$	m_{st}	η_{st}
First scenario	8.827	76.5	7	9	4	2
Second scenario	8.7	72.3	8	10	3	2

6. Optimization of Stiffeners

By applying GA for the mentioned scenarios, the near-optimal size for stiffeners in each scenario is obtained. Also, according to obtained n_{st} and m_{st} for each scenario, the appropriate ribs' angle can be calculated. Given the stiffener's size for each scenario, the total mass of the structure is also specified. All information is given in Table 3.

The introduced structure in the second scenario has less mass compared to the first one. So the stiffener size would be better in the second scenario, and the structure will have the minimum mass. According to the results, the optimum dimensions for stiffener buckling load for the optimal stiffener is equal to 1.3273 MPa which was increased by 80%.

7. Conclusions

In this study first buckling of the non-stiffened shell has been obtained and then the results were compared. The main theory of the problem is the linear first-order shear deformation theory. So at first, the buckling of a grid shell under these two theories is compared and then the effect of grid stiffeners on the buckling has been investigated. Then the effects of stiffeners' various parameters on the buckling of grid shells are discussed. In the end, the optimization of composite grid shells was designed using a Genetic Algorithm and the optimum parameters of stiffeners are introduced. According to the results, the buckling load for the obtained optimal stiffener has been increased by 80%.

Nomenclature

$\boldsymbol{z}$: Distance from the middle surface;
$\varepsilon_{ij}^{(0)}$: Middle surface normal strains;
$\gamma_{ij}^{(0)}$: Middle surface shear strains;
k_{ij} : Surface curvatures;
A_{st} : Cross-section area of stiffeners;
E_l : Longitudinal modulus of stiffeners;
c : $Cos\ \varphi$;
s : $Sin\ \varphi$;
F_{lz} : Force applied to the stiffeners;
N_{ij} : Resultant stress;
M_{ij} : Resultant momentums;
Q_{ij} : Stiffness coefficients;
h_k : The kth layer;
h_{k+1} : The (k+1)th layer;
S_{sh} : Equivalent stiffness matrix for shell;
S_{st} : Equivalent stiffness matrix for stiffeners;
U : Strain energy;
V : Potential energy;
M_i : Moments applied to unit cell;
G_{ij} : Shear modulus;
a : Length of unit cell;
b : Width of unit cell;
A_{ij}^{st} : Extensional stiffness of stiffeners;
B_{ij}^{st} : Coupling stiffness of stiffeners;
L_{ij} : Coefficient matrix;
H_{ij}^{st} : Shear stiffness of stiffeners;
$\bar{Q}_{ij}^{k}$: Reduced stiffness coefficients;
D_{ij}^{st} : Bending stiffness of stiffeners;

Conflicts of Interest

The author declares that there is no conflict of interest regarding the publication of this manuscript. In addition, the authors have entirely observed the ethical issues, including plagiarism, informed consent, misconduct, data fabrication and/or falsification, double publication and/or submission, and redundancy.

References

[1] Kim, C. G., Kang J.-H., 2005. Minimum-weight design of compressively loaded composite plates and stiffened panels for postbuckling strength by genetic algorithm, *Composite structures, 69* (2), pp.239-246.
[2] Kim, D. H., Choi D. H., and Kim, H. S., 2014. Design optimization of a carbon fiber reinforced composite automotive lower arm, *Composites Part B: Engineering, 58*, pp.400-407.
[3] Herath, M.T., Natarajan, S., Prusty, B.G., and John, N. St, 2014. Smoothed finite element and genetic algorithm based optimization for shape adaptive composite marine propellers, *Composite Structures, 109*, pp.189-197.
[4] Sekulski, Z., 2010. Multi-objective topology and size optimization of high-speed vehicle-passenger catamaran structure by genetic algorithm, *Marine Structures, 23*(4), pp.405-433.
[5] Kim, T.D., 2000. Fabrication and testing of thin composite isogrid stiffened panel, *Composite Structures, 49*, pp.21-25.
[6] Ambur, D. R., N. Jaunky, 2001. Optimal design of grid-stiffened panels and shells with variable curvature, *Composite Structures, 52*, pp.173-180.
[7] Zhang, Y.H., X.M. Qiu, D.N. Fang, 2008. Mechanical properties of two novel planar lattice structure, *Solid and Structures, 45*, pp.3751-768.
[8] Yazdani, M., Rahimi, G.H., 2010. The Effects of Helical Ribs' Number and Grid Types on

the Buckling of Thin-Walled GFRP Stiffened Shells under Axial Loading, *Journal of Reinforced Plastics and composite, 29*, pp.2568-2575.

[9] Jingxuan, H., Mingfa, R., Qizhong, H., Shanshan, S., & Haoran, C., 2011. Buckling behavior of compression-loaded advanced grid stiffened composite cylindrical shells with reinforced cutouts, *Polymers and Polymer Composites, 19*(4-5), 357-362.

[10] Vasiliev, V.V., Barynin, V.A., Razin, A.F., 2012. Anisogrid composite lattice structures–Development and aerospace applications, *Composite Structures, 94*, pp.1117–1127.

[11] Rahimi, G. H., Zandi, M., & Rasouli, S. F., 2013. Analysis of the effect of stiffener profile on buckling strength in composite isogrid stiffened shell under axial loading, *Aerospace Science and Technology, 24*, pp.198–203.

[12] Weber, J.M., Meddendorf, P., 2014. Semi-analytical skin buckling of curved orthotropic grid-stiffened shells", *Composite Structures, 108*, pp.616–624.

[13] Liu, Q., & Paavola, J., 2016. General analytical sensitivity analysis of composite laminated plates and shells for classical and first-order shear deformation theories, *Composite Structures, 127*, pp.88-101.

[14] Deveci, H. Arda, Levent Aydin, and H. Seçil Artem, 2016. Buckling optimization of composite laminates using a hybrid algorithm under Puck failure criterion constraint*, Journal of Reinforced Plastics and Composites, 35* (16), pp.1233-1247.

[15] Civalek O., 2016. Buckling analysis of composite panels and shells with different material properties by discrete singular convolution (DSC) method, *Composite Structures, 161*, pp.93–110.

[16] Ghasemi, A., Hajmohammad, M., 2017. Multi-objective optimization of laminated composite shells for minimum mass/cost and maximum buckling pressure with failure criteria under external hydrostatic pressure. *Struct Multidisc Optim 55*, pp.1051–1062.

[17] Hajmohammad, M., Tabatabaeian, A., Ghasemi, A., and Taheri-Behrooz, F., 2020. A novel detailed analytical approach for determining the optimal design of FRP pressure vessels subjected to hydrostatic loading: Analytical model with experimental validation, *Composites Part B: Engineering 183*, 107732.

[18] Ghasemi, A., Tabatabaeian, A., Hajmohammad, M., and Tornabene, F., 2021. Multi-step buckling optimization analysis of stiffened and unstiffened polymer matrix composite shells: A new experimentally validated method, *Composite Structures, 273*, 114280,

[19] Soltani, M., Abolghasemian, R., Shafieirad, M., Abbasi, Z., Amiri Mehra, AH., and Ghasemi, A., 2022. Multi-objective optimization of lateral stability strength of transversely loaded laminated composite beams with varying I-section*, Journal of Composite Materials 56*(12), pp.1921-1939.

[20] Khorshidi, K., Taheri, M., & Ghasemi, M. 2020. Sensitivity Analysis of Vibrating Laminated Composite Rec-tangular Plates in Interaction with Inviscid Fluid Using EFAST Method. Mechanics of Advanced Composite Structures, 7(2), 219-231.

[21] Arshid, E., Amir, S. and Loghman, A., 2021. Thermal buckling analysis of FG graphene nanoplatelets reinforced porous nanocomposite MCST-based annular/circular microplates. Aerospace Science and Technology, 111, p.106561.

[22] Reddy, J.N., 2004 *Mechanic of Laminated Composite Plates and Shells: Theory and Analysis* (Second Edition), CRC PRESS.

[23] Jaunky, N., N.F. Knight Jr, and D.R. Ambur, 1996. Formulation of an improved smeared stiffener theory for buckling analysis of grid-stiffened composite panels, *Composites Part B: Engineering, 27* (5), pp.519-526.

[24] Kidane, S., Li, G., Helms J., Pang S. S., and Woldesenbet E., 2003. Buckling load analysis of grid stiffened composite cylinders, *Composites Part B: Engineering, 34* (1), pp.1-9.

[25] Sadeghifar, M., Bagheri, M., and Jafari, A. A., 2011. Buckling analysis of stringer-stiffened laminated cylindrical shells with nonuniform eccentricity, *Archive of Applied Mechanics, 81*, pp.875-886.

[26] Shakib, M., 2007. Mechanics of Composite Structures (1), University of Imam Hussein press.

[27] Ghasemi, A.R. and Hajmohammad, M.H., 2015. Minimum-weight design of stiffened shell under hydrostatic pressure by genetic algorithm. Steel and Composite Structures, 19(1), pp.75-92.

[28] Ghasemi, A.R. and Hajmohammad, M.H., 2018. Mass and buckling criterion optimization of stiffened carbon/epoxy composite cylinder under external hydrostatic pressure. Latin American Journal of Solids and Structures, 15.

[29] Morozov, E. V., Lopatin, A. V., & Nesterov, V. A., 2011, Buckling analysis and design of anisogrid composite lattice conical shells, Composite Structures 93, pp.3150-3162.